Journal of Applied Sciences

ISSN 1812-5654

science alert

ANSInet
an open access publisher
http://ansinet.com

Journal of Applied Sciences 9 (21): 3843-3849, 2009
ISSN 1812-5654
© 2009 Asian Network for Scientific Information

Effects of Jet Hydraulic Properties on Geometry of Trajectory in Circular Buoyant Jets in the Static Ambient Flow

J. Ahadiyan and S.H. Musavi-Jahromi
Shahid Chamran University, Ahwaz, Iran

Abstract: In this study, governing equations of buoyant jets have been presented and drawdown trajectory of jet has been investigated. To achieve goals of this research program an extensive experimental study has been undertaken, a flume with 3.2 m length, 0.7 m width, 0.95 m height is constructed which is connected to a storage tank of dilute water from one side and a large concrete tank of fresh water on the other side in the Hydraulic Laboratory of Shahid Chamran University, Ahwaz, Iran. An extensive set of experiments was conducted, using different diffuser geometry and concentration of jet injection, to study downstream trajectory. Findings show that the length of jet trajectory decreases 10 up to 30% due to change of jet diameter from 5 to 8 mm. However, when the jet diameter increased from 8 to 15 mm, the length of trajectory showed 40% increased more than the observed length for jet diameter equal to 5 mm. Findings from this experimental study, shows that twice increase in concentration, causes positive length of flux buoyancy decrease 5 to 20%.

Key words: Round jet, trajectory, length, efflux momentum, density gradient

INTRODUCTION

According to the majority of researcher and especially environmental engineers, high-velocity flow from a buoyant jet represents an irrecoverable loss of power, for a basic axiom of hydraulics state that the entire kinetic energy of such a jet will be dissipated through reaction to the surrounding fluid (Albertson *et al*., 1950).

A concern with brine discharge from desalination plants is the increase in the near field salinity above the sea bed due to poor initial mixing (Del Bene *et al*., 1994). Along with the jet of desalination of dilution of the brine prior to discharge, the mixture of heat and salinity is also deliberately arranged to yield an almost neutrally buoyant discharge, so that the jet may not tend to sink, thus preparing the way to be pushed further out of the ambient flow. Turner (1967) and Kunze (1987) have investigated the salt fingering that has derived a downward salinity flux. Maxworthy (1983) and Turner (1998) have shown that a two-dimensional surface intrusion with a low Reynolds Number (R) will actually terminate its surface progression at the same distance and plunge downward. Ficher (1971) has suggested that the salt fingering flux can significantly be reduced by shear turbulence because of the disruption and reorientation of the salt fingers, although the degree of reduction has not yet been correlated to R in a quantitative manner. Turbulent discharges, initial mixing due to entrainment can be expected. The relative role of turbulence mixings and salt fingering need to be identified as well in order to determine whether and how the double diffusive mechanism can be included for the assessment of salinity increase near the below layer ambient fluid due to desalination discharges. Adrian and Stephan (2004) have investigated double diffusive effect on desalination discharge. Their study is divided into two experimental series. The first series included a surface rectangular jet, conducted with a fixed R of approximately 3500. The second series included a submerged round jet, performed with a higher R. Several researchers have recently tried to simulate mixing characteristics near and far from the field of jet by the numerical model. Somehow earlier Zhang and Adams (1999) had conducted numerical simulations, using the same far field model and had compared their simulations with predictions of a similar near field model under a range of conditions. While Kim *et al.* (2002) conducted jet integral-particle tracking model for single buoyant jets for both near and far field. Using the integral model, they simulated near field of jet flow and then modeled the advection-diffusion equation using the particle tracking method for far field process. Cuthberston *et al.* (2008) studied particle deposition process for the case of a round, turbulent, particle-laden, buoyant jet discharging horizontally into homogeneous receiving fluid that is initially either quiescent or coflowing. Ahadiyan and Musavi Jahromi (2008) have

Corresponding Author: Javad Ahadiyan, Faculty of Water Science Engineering, Shahid Chamran University, Ahwaz, Iran
Tel/Fax: 0098-0611-3365670

investigated variation of efflux momentum in shallow receiving water, using FLOW-3D and have shown that the momentum flux decreases in the longitudinal distance of jet position.

Buoyant jet is a kind of a free turbulence flow (Albertson *et al*., 1950). In this kind of flow, the velocity of the turbulence is proportional to the product of the mixing length and the mean velocity gradient. Schematic of longitudinal distribution of the jet velocity is shown in Fig. 1.

If the Reynolds Number for fluid efflux from a submerged boundary outlet is not too low, the mean velocity, v, at any point should depend only on the coordinates x,y and z on the efflux velocity v_0 and on a linear dimension, L_0. Thus dimensionless relationships between these parameters are:

$$\frac{v}{v_0} = f_1\left(\frac{x}{L_0}, \frac{y}{x}, \frac{z}{x}\right) \tag{1}$$

This relationship must be considered to involve the magnitude and the vector direction v the components of which may further be related through the differential continuity equation. The flux of flow Q past successive normal sections may be written as the integral of the differential flux v_x.dA over any normal section. Since, the entrainment Q will vary with the longitudinal distance x from the efflux section, its ratio to the efflux rate Q_0 may be written as follow:

$$\frac{Q}{Q_0} = \frac{\int_0^\infty v_x dA}{v_0 A_0} = f_2\left(\frac{x}{L_0}\right) \tag{2}$$

where, A_0 is the cross sectional area of the outlet. Similarly, since the momentum flux M may be written as the integral of the volume flux v_x.dA the longitudinal component of momentum per unit volume ρv_x, ρ, being

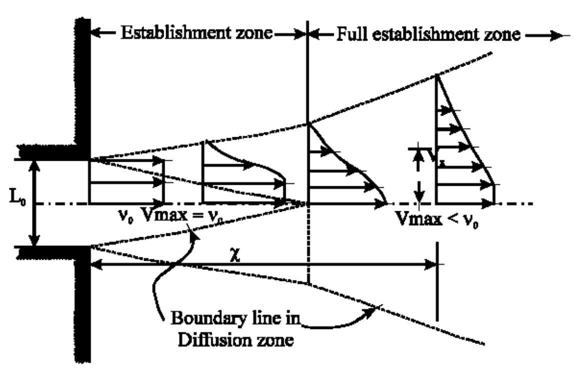

Fig. 1: Schematic representation of the jet diffusion (Alberston *et al*., 1950)

the fluid density, the ratio of M for any section to M_0 for the efflux section should be:

$$\frac{M}{M_0} = \frac{\int_0^\infty (v_x)^2 dA}{(v_0)^2 A_0} = f_3\left(\frac{x}{L_0}\right) \tag{3}$$

The hydrostatic force against jet flow causes the deceleration of the jet and the acceleration of the surrounding fluid is the tangential shear within the mixing region. Because this process is wholly internal, it follows at once that the momentum flux must be a constant for all normal sections of a given flow pattern:

$$\frac{M}{M_0} = \frac{\int_0^\infty (v_x)^2 dA}{(v_0)^2 A_0} = 1 \tag{4}$$

If, moreover, viscous action is presumed to have no influence on the mixing process, the diffusion characteristics and hence the characteristics of the mean flow should be dynamically similar under every condition.

In this study, hydraulic parameters and geometry of the trajectory in the buoyant round jets are investigated. Moreover, the trajectories under gradient of concentration carried out in quiescent ambient flow are also analyzed.

MATERIALS AND METHODS

In this study, geometry of the trajectories of round jet has been investigated using various discharges, concentration and diameter. To achieve this purpose, a physical model is constructed with a 3.2 m length, 0.7 m width and 0.95 m height in the Hydraulic Laboratory, Shahid Chamran University, Ahwaz, Iran (2007-2008). The schematic representation of flume and its equipments are shown in Fig. 2.

Figure 2 shows supply of fresh water from concrete storage tank by using pump with 20 L sec^{-1} and 15 m of head. The means of supply pump, experimental flume from fresh water is to be filled. Jet injection via salt density current is also transferred into experimental flume. Measurements include both length and height of trajectory under different jet injection concentrations, rate and temperature of jet injection. The program of experiments is shown in Table 1. In this Table 1, the jet properties and experimental schedule, at various cases, have been represented.

Dimensional analysis gives geometric and hydraulic characteristics of the jet flow in the static ambient fluid are function of Densimetric froude number (Adrian and Stephan, 2004; Pantokratoras, 2003) which is as follow:

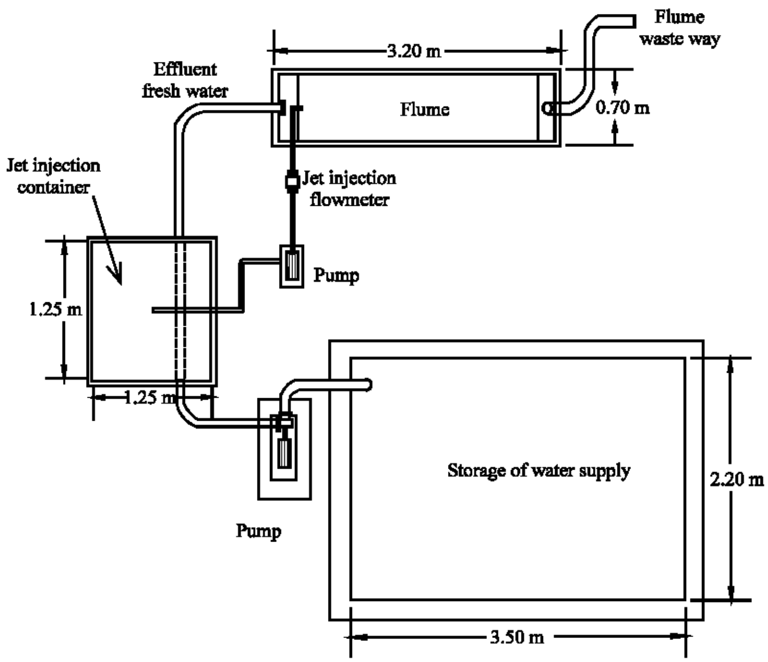

Fig. 2: Schematic of the experimental setup

Table 1: Scenarios in the experimental study

Concentration (g L^{-1})	Diameter (mm)	Discharge (L sec^{-1})	Concentration (g L^{-1})	Diameter (mm)	Discharge (L sec^{-1})
15	5	0.014	30	5	0.014
		0.026			0.026
		0.037			0.037
		0.048			0.048
	8	0.026		8	0.026
		0.053			0.053
		0.078			0.078
		0.110			0.110
	15	0.810		15	0.810
		0.175			0.175
		0.278			0.278
		0.375			0.375

$$Fr_j = \frac{V_0}{\sqrt{\frac{\Delta\rho}{\rho_a}.g.d_p}} \tag{5}$$

In Eq. 5 V_0 is efflux velocity, $\Delta\rho$ is density gradient between jet injection and ambient fluid, g is acceleration due to gravity, dp is jet diameter. In addition to Densimetric Froude Number, there is another parameter as X/dp which X is length of positive buoyancy (Pantokratoras, 2003).

As shown in Table 1, several scenarios are considered to be investigated. The first part of scenarios is for 15 g L^{-1} of salinity. In the second part of scenarios, 30 g L^{-1} of salinity is chosen. Three diameters including 5, 8 and 15 mm of round jet, are considered. All experiments have been performed with 3 jet diameters and 4 discharges. Jet injection velocity in efflux section determined 0.5, 1, 1.5 and 2 m sec^{-1}. The entire experiments performed in constant thermal condition between jet injection and ambient flow due to same condition for heat transferring. The temperature of jet injection kept constant equals to 25°C. In all experimental works the temperature was read using a digital thermometer with 0.1°C accuracy. Besides the fluid density was measured with a hydrometer 151 H standardized was carried out with ASTM Standard E100 (2003) method, respectively. In this study, several experiments have been undertaken using salt water with different density.

RESULTS

In this study program, different discharges, various concentration of jet and several diffusers geometry were selected. The trajectory affect on two phases flow density gradient in some way (x,z) coordination measured. Because of unchangeable the y coordinates and its symmetry to bases jet core was not measured. Rate of jet injection was measured using electromagnetic flowmeter (with 0.2% accuracy). The density of jet injection and surrounding fresh water was calculated and measured by means of standardized hydrometer 151 H ASTM (ASTM Standard E100, 2003). The mixing pump (with 18 m height and 2.5 L sec^{-1} discharge) had the function of recycling density current storage so as to keep the jet injection homogeneous. The result of trajectory affect jet properties

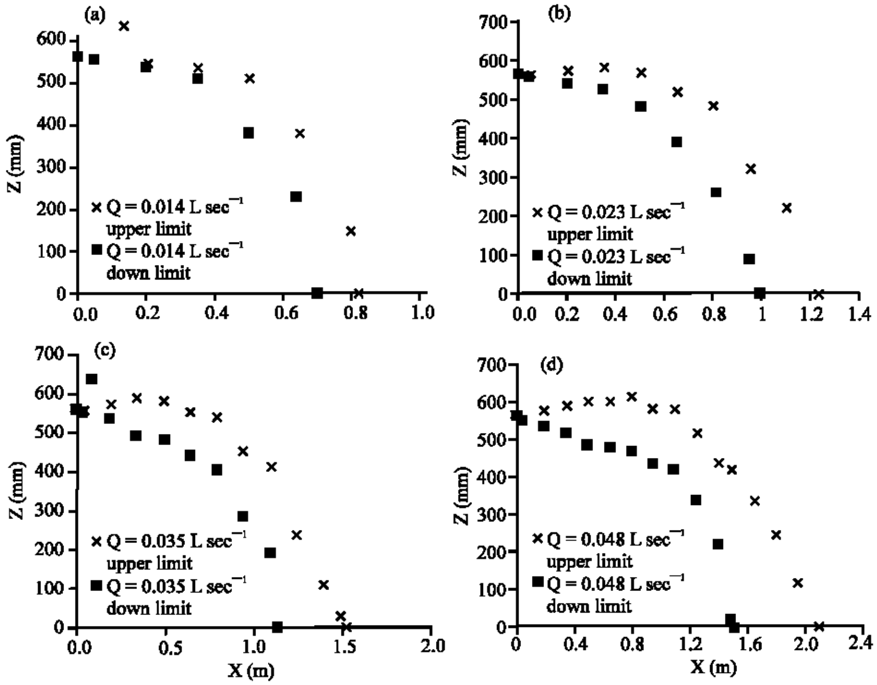

Fig. 3: Jet trajectory in the fresh water (Dia. = 5 mm and Conc. = 15 g L^{-1}). (a) Q = 0.014 L sec^{-1}, (b) Q = 0.023 L sec^{-1}, (c) Q = 0.035 L sec^{-1} and (d) Q = 0.047 L sec^{-1}

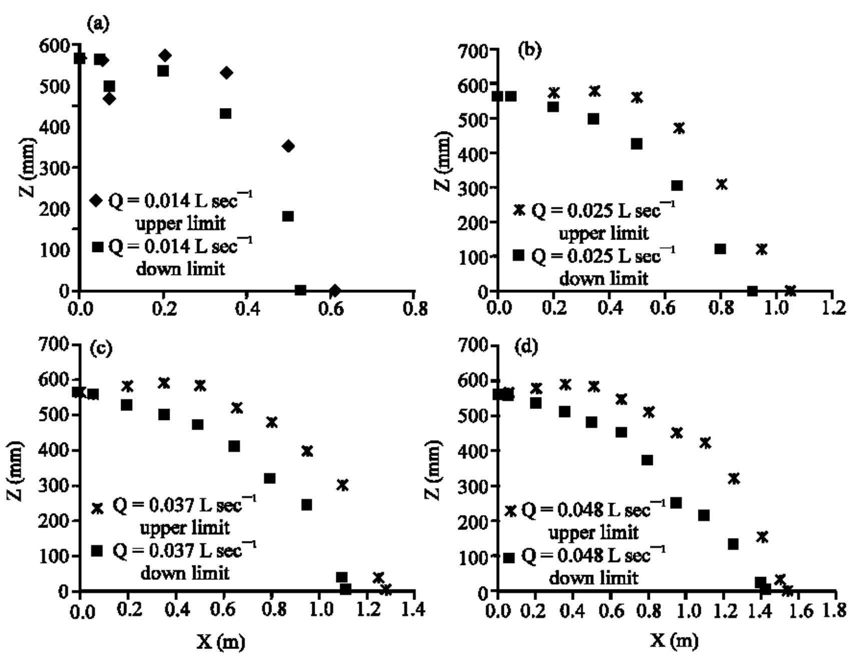

Fig. 4: Jet trajectory in the fresh water (Dia. = 5 mm and Conc. = 30 g L^{-1}). (a) Q = 0.014 L sec^{-1}, (b) Q = 0.023 L sec^{-1}, (c) Q = 0.035 L sec^{-1} and (d) Q = 0.047 L sec^{-1}

for 5 mm diffuser diameter and salt concentration of jet injection equal 15 g L^{-1} is shown in Fig. 3. Trajectories due to different effluent discharge are shown in Fig. 4.

As shown in Fig. 3, the length of trajectory is increased for higher effluent discharge. The trajectory affect from jet properties such as the other jet geometry

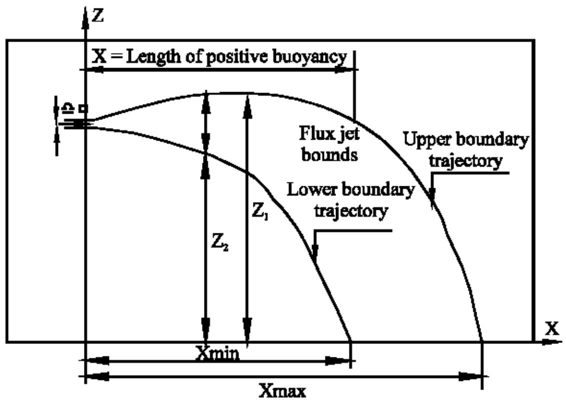

Fig. 5: Schematic of a trajectory and its upper and lower boundaries

Table 2: Result of trajectory length regarding to experimental study

C ($g\ L^{-1}$)	V ($m\ sec^{-1}$)	D = 5 mm Xmax (m)	D = 5 mm Xmin (m)	D = 8 mm Xmax (m)	D = 8 mm Xmin (m)	D = 5 mm Xmax (m)	D = 5 mm Xmin (m)
15	0.5	0.82	0.70	0.59	0.44	0.94	0.82
	1.0	1.23	0.99	1.14	0.98	1.42	1.23
	1.5	1.53	1.14	1.48	1.33	1.75	1.50
	2.0	2.10	1.52	1.85	1.60	1.88	1.68
30	0.5	0.61	0.53	0.57	0.47	0.58	0.52
	1.0	1.05	0.92	0.99	0.82	1.10	0.95
	1.5	1.28	1.12	1.42	1.28	1.68	1.26
	2.0	1.70	1.42	1.95	1.68	2.00	1.69

Table 3: Densimetric Fruode Number an relative length of positive buoyancy (C = 15, 30 g L^{-1})

Di/dp	dp mm	Q_0 L sec^{-1}	$Fr_j\ C_1$	X/dp C_1 Positive buoyancy	$Fr_j\ C_2$	X/dp C_2 positive buoyancy
5.08	5	0.014	32.50	37.27	21.97	46.00
		0.023	53.40	105.26	43.94	85.52
		0.037	85.91	137.94	65.52	132.59
		0.048	111.45	228.24	79.42	170.12
3.18	8	0.026	18.64	25.00	14.61	26.49
		0.053	38.00	64.48	27.66	59.71
		0.078	55.93	104.40	42.27	101.83
		0.110	78.87	152.20	57.40	145.90
2.54	15	0.078	11.62	23.94	7.91	17/15
		0.176	26.21	50.64	18.75	42.89
		0.279	41.55	66.38	30.35	61.23
		0.368	54.18	91.81	40.65	82.90

(8 and 15 mm diffuser diameter) and concentration salt density current equal 30 g L^{-1} is calculated. For example, results of trajectories affect of jet properties for 5 mm diffuser diameter and salt concentration of jet injection equal 30 g L^{-1} is represented in Fig. 4.

The observed data in research program including z_1, z_2, Xmax and Xmin were measured. Schematic of a trajectory and its characteristics is presented in Fig. 5. Then, dependent variables including; densimetric froude number and X/dp are calculated. Variation of the length of positive buoyancy is the main cause for variation of the Xmin and Xmax. Observed upper (z_1) and lower (z_2) limits of trajectory in vertical direction are recorded. Variation of z_1 and z_2 affect the length of positive buoyancy. Findings show that increase of jet injection concentration or increasing density of jet injection will significantly affect the length of trajectory which is shown in Fig. 3 and 4. The entire differences of trajectory length interaction of both geometry and concentration of jet injection are reported in Table 2. Table 3 shows Densimetric Froude Number and X/dp due to different concentration of jet flow and different diameter of jet efflux.

DISCUSSION

Adrian and Stephan (2004) investigated double diffusive effect on desalination discharge and present an equation for trajectory and its straight length downstream. In the present study, positive buoyancy length of trajectory for upper and inferior limits due to simultaneous jet geometry, fluid concentration and different diameters were studied. Adrian and Stephan performed their study in the low Reynolds Number, but higher Reynolds Number which already was not considered has been carried out in the present study. As shown in Table 4, Adrian and Stephan found the straight length of trajectory which is affected by the positive buoyancy zone, is less than findings of the present study. Comparing with observed data the present study showed more accuracy than Adrian and Stephan (2004). It is due to the effect of geometry on the positive buoyancy length.

Density difference in the jet flow and ambient fluid causes the diffusion of jet in the ambient fluid. While jet fluid injection into air (no buoyant jet) does not shows this kind of diffusion. Thus two values for Z direction were recorded and calculations for the upper and lower boundaries were drowned. In Table 2 Xmax and Xmin are related to the final trajectory length which are equal to the maximum length for the upper boundary and lower boundary curves, respectively, as shown in Fig. 2. In general calculation for buoyancy forces shows two regions. The first region has positive buoyancy causing the upper boundary of jet trajectory showing an increasing depth relative to jet axis, which is more pronounced for lower densities. Also, with increasing injection velocities due to increasing friction resistance and pressure gradient, positive buoyancy values will be greater. In this second region, negative buoyancy forces are more prominent so that the injection fluid density relative to the buoyancy and hydrodynamic forces are

Table 4: Comparison of present study with Adrian and Stephan (2004) findings

Reynolds No. of jet	Adrian and Stephan double diffusive on fluid	Present study geometry jet and concentration fluid
	($X\ dp^{-1}$)	
Re<6000	42	37.00
	28	53.50
	17	25.00
	28	46.00
	21	85.00
	15	26.50
6000<Re<10000	80	64.48
		91.81
	64	132.52
		59.71
	55	82.90
		98.50
Re>10000	-----	228.24
		104.40
		152.20
		91.38
		170.12
		101.83
		145.90
		82.90

greater causing the downward trajectory of the jet. In this region, complete mixing between of jet fluid and injected fluid due to the spreading jet influx. Experimental results show that $\Delta\rho/\rho_a$ equal 0.00981 and 0.01852 for concentration 15 and 30 g L^{-1} consequently. The results show that Densimetric Fruode number is decreased with increasing in concentration, as a result relative length of buoyancy is decreased, which is due to balance between frictional forces and momentum forces. Findings show that the lengths of jet trajectory decreases 10 up to 30% due to change of jet diameter from 5 to 8 mm. The main reason being the decrease of friction forces resulting in allays hydrodynamics forces. On the contrary, when the jet diameter increased to 15 mm, the length of trajectory showed 40% increased more than the observed length for the jet diameter equals to 5 mm. This object occurs due to the domination of momentum forces from buoyancy and drag forces both. The momentum forces in bigger diffuser exceeded smaller diffuser wherefore the volume jet injection in this condition would highly increase.

The resultant buoyancy, friction and momentum forces have a great effect on the total trajectory length. According to the result obtain buoyancy forces depend on concentration of jet fluid and flux dimension, friction forces depend on flux frontal surface and the momentum forces depend on efflux velocity and jet geometric parameter. Forces analysis shows that the 8 mm diameter jet has a shorter total trajectory length compare to other diameters and for 15mm diameter jet, the maximum total trajectory length is achieved due to an increasing in forward pushing forces relative to the buoyancy and friction forces.

CONCLUSIONS

On the basis of experiments and several computations can be concluded: Length of jet trajectory decreases 10 up to 30% due to change of jet diameter from 5 to 8 mm. Length of jet trajectory of the bigger diffuser (15 mm) is increased even 40% rather than smaller diffuser. Analysis shows that length of trajectory decrease from 0 to 40% due to twice concentration. Analysis shows that the 8 mm jet diameter has a shorter trajectory length compare to other diameters and for 15 mm jet diameter, the maximum total trajectory length is achieved due to an increasing in forward pushing forces relative to the buoyancy and friction forces.

ACKNOWLEDGMENTS

This study program is conducted under contract No. 88-01-02-001 with Khuzestan Water and Power Authority. The financial support of the Khuzestan Water and Power Authority is acknowledged. Shahid Chamran University support to the first author as Ph.D candidate is also appreciated.

REFERENCES

Adrian, W.L. and G.M. Stephan, 2004. Double diffusive effect on desalination discharges. J. Hydraulic Eng., 130: 450-457.

Ahadiyan, J. and S.H. Musavi Jahromi, 2008. Investigation of variation of efflux momentum in shallow receiving water by using FLOW-3D. Proceeding of the International Symposium of Water Resource Management, Tabriz, Iran, (ISWRMT'2008), pp: 551-557.

Albertson, M.L., Y.B. Dai, R.A. Jenson and H. Rouse, 1950. Diffusion of submerged jets. Trans. Am. Soc. Civil Engrg., 115: 639-664.

ASTM Standard E100, 2003. Standard Specification for ASTM Hydrometers. ASTM International, West Conshohocken, PA.

Cuthberston, J.S., A. Peter and P.A. Davis, 2008. Deposition from particle-laden round turbulent horizontal buoyant jets in stationary and coflowing receiving fluids. J. Hydraulic Eng., 134: 390-402.

Del Bene, J.V., G. Jirka and J. Largier, 1994. Ocean brine disposal. Desalination, 97: 365-372.

Fischer, H.B., 1971. The dilution of an undersea sewage cloud by salt fingers. Water Res., 5: 913-915.

Kim, Y.D., S.W. Kang, I.W. Seo and B.C. Oh, 2002. Modeling the mixing of wastewater effluent discharged from ocean outfalls using a hybrid model. Coastal Eng. J., 43: 259-288.

Kunze, E., 1987. Limits on growing finite-length fingers a richardson number constraint. J. Mar. Res., 45: 533-556.

Maxworthy, T., 1983. The dynamics of double diffusive gravity currents. J. Fluid Mech., 128: 259-282.

Pantokratoras, A., 2003. Vertical penetration of double diffusive water plumes discharged vertically downward. J. Hydraulic Eng., 129: 541-545.

Turner, J.S., 1967. Salt fingers a density interface. Deep-Sea Res., Oceanogr. Abstr., 14: 599-611.

Turner, J.S., 1998. Stratification and circulation produced by heating and evaporation on a shelf. J. Mar. Res., 56: 855-904.

Zhang, X.Y. and E.E. Adams, 1999. Predication of near field plume characteristics using field circulation model. J. Hydraulic Eng., 125: 233-241.